Computational Modeling of a Piezoelectrically Actuated Microvalve for the Control of Liquid Flowrate

S. M. Saeidi*, J. M. Khodadadi*, C. A. Johnson*, C. Lee** and E-H Yang**

*Mechanical Engineering Department, Auburn University
201 Ross Hall, Auburn, AL, USA, 36849, khodajm@auburn.edu
**NASA JPL, Pasadena, CA, USA, eui-hyeok.yang@jpl.nasa.gov

ABSTRACT

Computational modeling of liquid flow in a piezoelectrically actuated microvalve is discussed. A 3-D structured mesh with 330,000 hexahedral cells that represents the major features of the microvalve was generated for the numerical model. Due to the symmetry of the microvalve about two planes, only one-fourth of the microvalve was modeled. The mesh is denser in the regions which experience excessive pressure drop. The commercial CFD code FLUENT was utilized for the solution of the continuity and momentum equations. The three-dimensional velocity and pressure fields were obtained. By changing the mass flow rate at the inlet, the pressure drop between the inlet and outlet ports is found and a loss coefficient is determined for every deflection. The predicted pressure drop values are compared to the experimental data for water flow within the microvalve.

Keywords: microfluidics, microvalve, modeling, CFD, liquid flow.

1 INTRODUCTION

Microvalves that are compatible with both liquids and gases will be integral parts of proposed micropropulsion units for microspacecrafts and microsatellites. The design, operation and performance of such a leak-tight piezoelectrically actuated microvalve for high-pressure gas micropropulsion was recently reported [1]. In the process of enhancing this class of microvalves, a leak-tight, low-power, liquid-compatible, piezoelectrically actuated microvalve has been designed, fabricated, and characterized. The microvalve consists of a custom-designed piezoelectric stack actuator bonded onto silicon valve components. The microvalve has a silicon membrane called boss plate (Figure 1) for isolating the piezoelectric actuator from the liquid effluents. The valve seat configurations include narrow-edge 12 seating rings and tensile-stressed silicon tethers that enable the normally closed and leak-tight operation. A concentric series of narrow rings (Figure 2) simulate a "knife-edge" seal by reducing the contact area, thereby increasing the seating pressure and consequently reducing internal leaks [2].

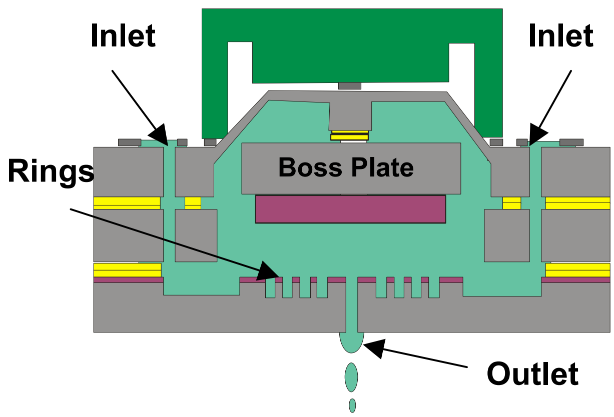

Figure 1: Operating principle of the microvalve in actuated "on" state.

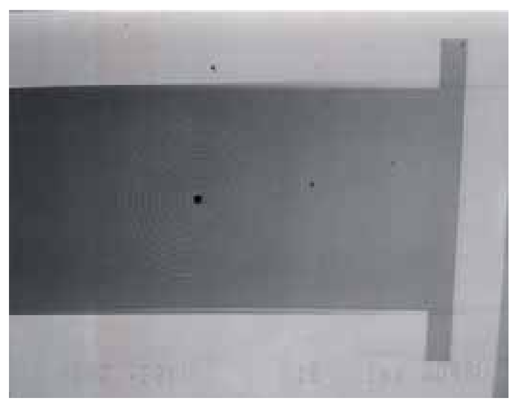

Figure 2: SEM image of the valve seat, concentric rings and outlet hole.

2 GEOMETRY OF THE MICROVALVE MODEL

The geometry of the modeled microvalve is shown in Figure 3. The flow enters the microvalve from four inlet pipes positioned at the corners of the upper boss plate and exits the valve from an outlet hole fabricated at the middle of the seat plate. The diameter of the inlet and outlet pipes is 200 microns. The length of the inlet pipes is 7100 microns whereas the length of the outlet pipe is 600 microns. The liquid enters a 10-micron high box after

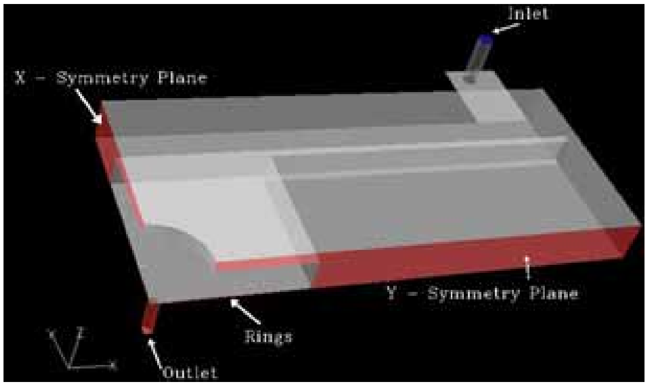

Figure 3: A quarter of the microvalve.

passing through the inlet pipe and then flows into a bigger box with 6 × 5.2 × 0.56 millimeters dimensions. There are twelve thin seat rings with different radii that surround the outlet hole. The thickness of the rings is 1 micron and their height is 10 microns. The diameter of the first surrounding ring is 110 microns and other rings are evenly placed with a 150 microns distance from each other. There is a moving square-shape lower boss plate on top of the outlet hole and rings with the dimensions of 1.8 × 1.8 × 0.4 millimeters. The flow is directed to the outlet pipe after passing through the space between the lower boss plate and the rings. Passage of the flow through this narrow gap causes most of the pressure drop in the system along with the small box under the inlet pipe. The spacing between the lower boss plate and the seat plate ranges from 11 to 13.5 microns, which means the distance between the tip of the rings and lower boss plate varies from 1 to 3.5 microns, respectively. Three models for deflections of 1, 2.7, and 3.5 microns were studied.

3 PROBLEM FORMULATION

A 3-D structured mesh with 330,000 hexahedral cells that represents the major features of the microvalve was generated (Figure 4) for the numerical model. Due to the symmetry of the microvalve about two planes, only one-fourth of the microvalve was modeled. The mesh is denser in the regions that experience excessive pressure drop (between the boss and seat plates and where the flow enters the microvalve). The continuum based momentum and continuity equations are valid for this problem [3]. The flow is laminar, incompressible, and steady. The governing equations of continuity and momentum in tensor notation form are:

$$\frac{\partial u_i}{\partial x_i} = 0 \tag{1}$$

$$\frac{\partial}{\partial x_j}\left(\rho u_i u_j\right) = -\frac{\partial p}{\partial x_i} + \mu \frac{\partial}{\partial x_j}\left(\frac{\partial u_i}{\partial x_j} + \frac{\partial u_j}{\partial x_i}\right) \tag{2}$$

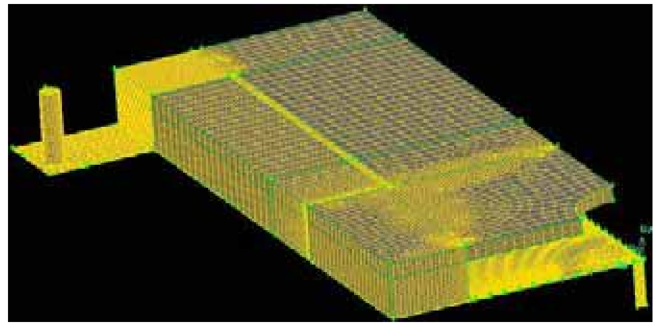

Figure 4: Three-dimensional mesh used for CFD analysis.

The version 6.2 of the commercial code FLUENT was utilized for solving the governing equations. The no-slip boundary condition was chosen for the walls whereas symmetry boundary condition was used on the symmetry planes. The second order upwind scheme was chosen to discretize the momentum equations whereas the SIMPLE algorithm is used to couple the pressure and velocities. Two different types of boundary conditions were applied to the inlet and outlet ports. At first, a gage stagnation pressure was specified at the inlet port and the outlet pressure was set to zero (gage). In order to verify the results, the mass flow rate of the system that was found by applying the above boundary conditions, was chosen as the inlet boundary condition and flow at the outlet was assumed fully developed. The problem was solved again with the assigned boundary condition. The same stagnation pressure was found at the inlet. A total of 15 cases were run for 3 deflections of 1, 2.7 and 3.5 microns and 5 inlet stagnation pressures of 3, 5, 10, 15 and 20 psi. The working liquid is water.

4 RESULTS AND DISCUSSION

In Figure 5, the pathlines are shown for the case with 2.7 microns deflection. The pathlines are released at the inlet plane from two rake sets that are placed normal to each other (Figure 6).

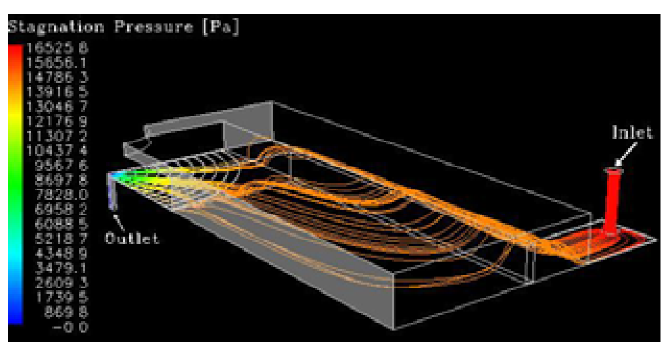

Figure 5: Pathlines released at inlet.

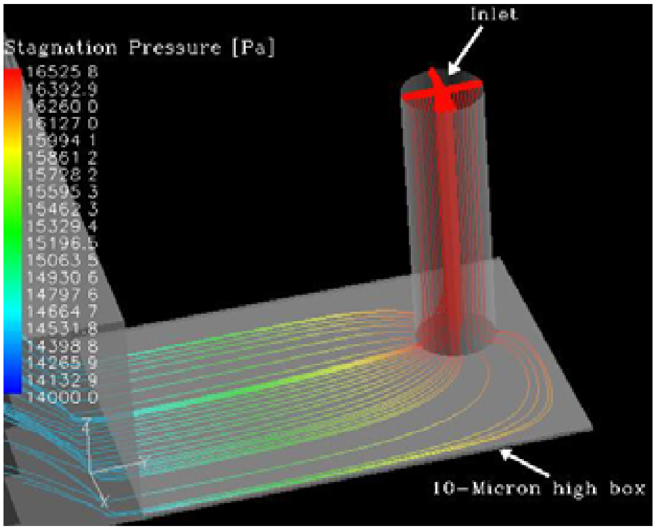

Figure 6: Pathlines colored by stagnation pressure in the inlet pipe and 10-micron box.

The pathlines released from these rakes are colored by the local stagnation pressure values. The fluid particles prefer to flow over the tether rather than beneath it due to the lower resistance offered. Pressure is almost constant in the inlet pipe but suddenly drops markedly where the flow faces the normal plate that is located 10 microns away from the exit of the inlet pipe. Once the flow emerges into the microvalve cavity, pressure remains almost constant until the flow passes over the rings in the gap between the seat and the boss plates. The pressure monotonically decreases as the flow passes over each ring (Figure 7).

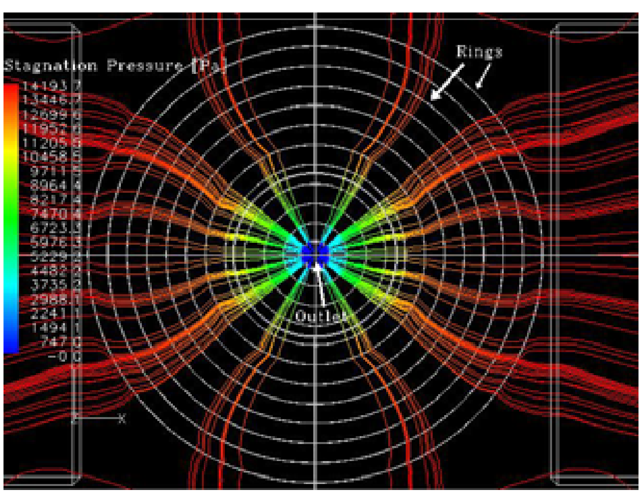

Figure 7: Pathlines colored by stagnation pressure over the rings and the outlet hole.

Since most of the pressure drop occurs across the rings, a 2-D axisymmetric analysis was performed on the geometry in and around the rings. The pressure drop found from the 2-D analysis verifies the accuracy of the 3-D model results. Pressure drop versus mass flowrate results are compared between the numerical (2-D and 3-D) and experimental data for a 1-micron deflection in Figure 8. The observed trend for the numerical results is a straight line that passes through the origin. The results based on utilization of both boundary conditions are in accordance with each other. The experimental results lie between the 2-D and 3-D results. The experimental data are close to 2-D results at low inlet pressure cases but for the cases with high pressure at the inlet, the experimental data tend toward 3-D results.

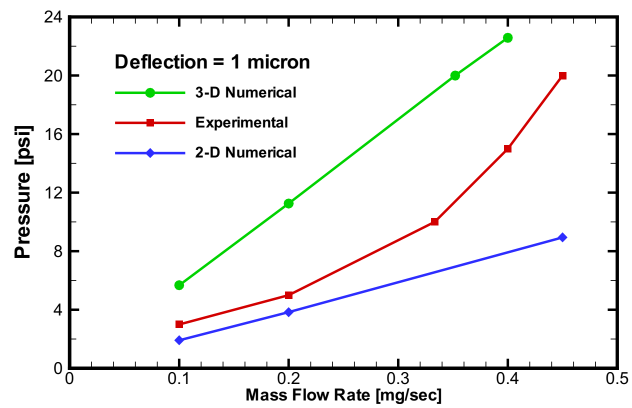

Figure 8: The comparison among two- and three-dimensional numerical results and experimental data.

In Figure 9, 3-D numerical results for pressure drop versus mass flowrate are shown for deflections of 1, 2.7 and 3.5 microns. For a constant pressure difference, the mass flow rate increases as the deflection increases. The values of the pressure drop coefficient, K versus deflection are shown in Figure 10. The pressure drop coefficient is defined as the slope of the lines in Figure 9. Figure 10 shows that K has a logarithmic relationship with deflection, and is therefore very sensitive to changes in deflection.

5 CONCLUSIONS

1. The mass flow rate varies linearly with pressure difference. This is expected because the flow is in the low range of Reynolds numbers with the highest value being 6.

2. The results indicate the sensitivity of the pressure drop coefficient to deflection. Small change in deflection can greatly modify the value of K. Therefore, the differences between the numerical and experimental results

can be explained in view of the tolerance of the measured deflections.

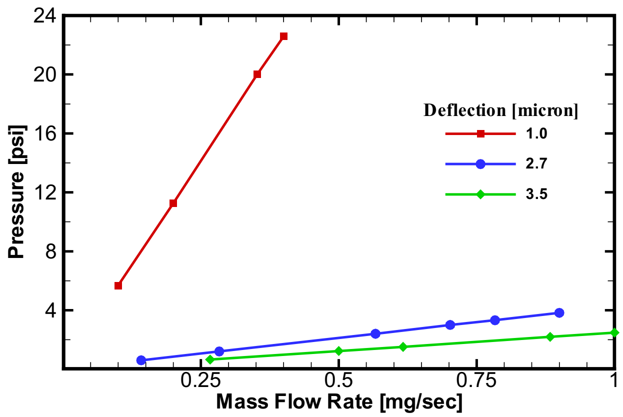

Figure 9: The comparison among three-dimensional numerical results with different deflections.

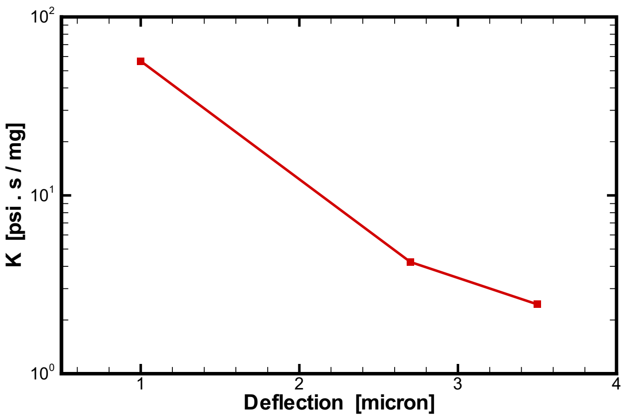

Figure 10: Pressure drop coefficient for different deflections.

ACKNOWLEDGMENT

C. A. Johnson acknowledges the support of the Alabama Space Grant Consortium, NASA Training Grant NGT5-40077.

REFERENCES

[1] E-H Yang, C. Lee, J. Mueller and T. George, "Leak-Tight Piezoelectric Microvalve for High-Pressure Gas Micropropulsion," Journal of Microelectromechanical Systems, Vol. 13, No. 5, pp. 799-807, 2004.

[2] C. Lee and E-H Yang, "Piezoelectric Liquid-Compatible Microvalve for Integrated Micropropulsion," Solid State Sensor, Actuator and Microsystems Workshop, Hilton Head Island, South Carolina, June 6-10, 2004.

[3] G. E. Karniadakis and A. Beskok, "Micro Flows: Fundamentals and Simulation," Springer, 2001.